

Article

Effects on Greenhouse Gas (CH₄, CO₂, N₂O) Emissions of Conversion from Over-Mature Forest to Secondary Forest and Korean Pine Plantation in Northeast China

Bin Wu ^{1,2}  and Changcheng Mu ^{1,2,*}

¹ Center for Ecological Research, Northeast Forestry University, No.26 Hexing Road Xiangfang District, Harbin 150040, China; wb_heb@126.com

² Ministry of Education Key Laboratory of Sustainable Forest Ecosystem Management, Northeast Forestry University, No.26 Hexing Road Xiangfang District, Harbin 150040, China

* Correspondence: muccks@nefu.edu.cn

Received: 14 August 2019; Accepted: 9 September 2019; Published: 11 September 2019



Abstract: This study aimed to evaluate the seasonal variations of Greenhouse Gas fluxes (CH₄, CO₂, and N₂O), Greenhouse Gas (GHG) emissions, and Global Warming Potential (GWP) over the extent of the regions and understand the controlling factors. CH₄, CO₂, and N₂O fluxes were measured along with their environmental variables from the over-mature forest, Korean pine plantation, and five 60-year-old natural secondary forests in mountainous regions in Northeast China from May 2015 to April 2016. The results revealed that secondary forests, except for *Betula platyphylla* forest, significantly increased CH₄ absorption by 19.6% to 51.0% and 32.6% to 67.0% compared with over-mature forest (OMF) and Korean pine plantation (KPP). Five secondary forests significantly increased CO₂ flux by 32.9% to 78.6% and 14.1% to 53.4% compared with OMF and KPP, respectively. According to the annual statistics, the N₂O fluxes had significant differences among seven forest types and decreased in the following order: mixed deciduous forest (MDF) > OMF > KPP > *Populus davidiana* forest (PDF) > hardwood forest (HWF) > Mongolian oak forest (MOF) > *Betula platyphylla* forest (BPF). The CH₄ absorption and CO₂ emission peaks occurred in summer, while the peak N₂O fluxes occurred in spring. Stepwise multiple linear regression showed that CH₄ and CO₂ fluxes from soils were strongly influenced by air and soil temperature, soil volumetric water content (SVWC), nitrate nitrogen (NO₃⁻-N), ammonium nitrogen (NH₄⁺-N), and soil organic carbon (SOC) across the whole year. Air temperature, SVWC, pH, NO₃⁻-N, and NH₄⁺-N were the dominant factors controlling N₂O fluxes from OMF and five secondary forests (except for BPF). No significant relationships were observed between these environmental factors and N₂O fluxes from KPP and BPF. Additionally, the total cumulative CH₄, CO₂, and N₂O fluxes were -13.37 t CH₄ year⁻¹, 41,608.96 t CO₂ year⁻¹, and 3.24 t N₂O year⁻¹, and the total cumulative GWP were 42,151.87 t CO₂ eq year⁻¹ through the whole year in seven forest types at the Maoershan Ecosystem Research Station in Northeast China. For the annual GWP per hectare, secondary forests and KPP averaged a higher GWP by 33.7%–80.1% and 17.9% compared with OMF. This indicates that the effects of early human activities have not been completely eliminated in the middle stage of KPP and secondary forests.

Keywords: secondary forests; over-mature forests; Korean pine plantation; greenhouse gas fluxes; global warming potential

1. Introduction

The emissions of Greenhouse Gases (GHGs), such as CH₄, CO₂, and N₂O, are a natural phenomenon that has been recognized to contribute to more than 90% of the anthropogenic climate warming [1]. According to the 2013 Intergovernmental Panel on Climate Change (IPCC) assessment, atmospheric concentrations of these gases have exceeded the pre-industrial levels by 40%, 150%, and 20%, respectively [2]. Additionally, they have already raised the global average surface temperature by 0.39 °C (0.69–1.08 °C) between 1901 and 2012 [3]. Although many studies consider CO₂ to be the most important greenhouse gas, CH₄ and N₂O also play major roles in terrestrial ecosystems [4,5]. Forest soils have been identified to be a significant sink for atmospheric CH₄, and it is estimated that CH₄ uptake activities of soils represent 3%–9% of the global atmospheric CH₄ sinks [6]. It has also been identified as a significant source for N trace gases, accounting for 60% of the total annual N₂O emissions [7,8]. Additionally, with a span of 100 years, the global warming potential of CH₄ and N₂O is 28 and 265 times that of CO₂, respectively [9]. However, few researchers simultaneously observed all three greenhouse gases over a full year in the temperate region of Asia, and thus a comprehensive study into the exchanges of CH₄, CO₂, and N₂O between terrestrial ecosystems and the atmosphere is much needed.

The forest ecosystem plays a crucial role in regulating the atmospheric GHG concentration, especially after conversion from over-mature forest to secondary forest and plantations; the forest ecosystem can greatly affect soil GHG fluxes due to the variability of vegetation by altering the critical biogeochemical cycling of C and N and microbial activity [10]. However, the impact of forest conversion on GHG emissions remains uncertain: some studies have shown that it increases the seasonal emission of CO₂ and uptake of CH₄ [11], decreases N₂O emission [12], or increases CH₄ emission [13]; a study by Maljaned et al. [14] also revealed no effect on GHG emissions or uptakes. These differences are mainly due to the variations in tree species and vegetation composition, as well as soil chemical and physical properties such as texture, temperature, water content, and nutrient content [15]. The variability of vegetation in forests leads to the changes in the biogeochemical cycling of C and N and microbial activities. Therefore, natural secondary forest and plantations can greatly affect soil GHG fluxes. More attention should be paid to the influence of secondary forest and plantations on GHG emissions, which could help to improve the understanding of their effects on climatic variation [16].

The CH₄, CO₂, and N₂O fluxes are strongly controlled by multiple factors, including air and soil temperature, soil volume water content, vegetation, and substrate availability [4,17,18]. Specifically, CH₄ fluxes are the result of the balance between production and consumption [19]. Soil organic matter decomposition and respiration by litter and roots contribute to CO₂ emissions [20]. N₂O is mainly produced in soils because of two microbial activities: microbial nitrification (aerobic conditions) and denitrification (anaerobic conditions) [21]. The CH₄, CO₂, and N₂O fluxes have rather large variations due to the complex processes of GHG fluxes and the variability of their controlling factors [4]. Therefore, exploring the main factors which play a decisive role in influencing GHG emissions is becoming increasingly critical.

The temperate mixed forest in East Asia ranks with that in northeastern North America and Europe as three largest portions of temperate mixed forests in the world. The temperate forest in Northeast China, as the predominant distribution area for the Asian temperate mixed forest, accounts for 35.3% and 34.5% of forested area and standing tree volume in the whole nation, respectively [22,23]. Since the turn of the 20th century, the Chinese government, Russians, and Japanese have destroyed the pristine forests by large-scale industrial logging. Subsequently, the pristine forests were replaced by secondary forests and plantations [24]. Smith et al. [25] indicated that land use practices have a significant influence on the environmental factors controlling GHG fluxes, and thus GHG fluxes. Therefore, the contribution of GHG fluxes to the global warming potential (GWP) might be changed in different land use types; to reveal the influence of forest types on GWP and regulate it, it is necessary to quantify how much each forest type contributes to GWP. However, studies on the contribution of different forest types to GWP are still limited. Thus, the representative forest conversion sequence with

a clear land-use history, located at the Maoershan Ecosystem Research Station of Northeast Forestry University in Northeast China, provides an excellent opportunity to conduct valuable research on the evaluation of GHG emissions and GWP among the over-mature forest, secondary forest, and Korean pine plantation in the study region.

The objectives of the present study are (1) to identify the main factors controlling the GHG variations; (2) to evaluate GHG emissions and GWP in different land uses at the Maoershan Ecosystem Research Station of Northeast Forestry University in Northeast China. In order to achieve these objectives, CH₄, CO₂, and N₂O fluxes were measured monthly from May 2015 to April 2016. Additionally, the air and soil temperature, soil volumetric water content (cm³ H₂O cm⁻³ soil), soil pH, soil N content (NO₃⁻ and NH₄⁺), and soil organic carbon were also measured. The results are useful for estimating the influence of conversion from over-mature forest to secondary forest and Korean pine plantation on GHG changes and GWP.

2. Materials and Methods

2.1. Study Area

Field experiments were conducted from May 2015 to April 2016 at the Maoershan Ecosystem Research Station of Northeast Forestry University in Northeast China (45°20′–25′N, 127°30′–34′E; 300 m.a.s.l.). The region represents typical forest types and landscape in Northeast China with a dark brown forest soil, and the parent material is granite bedrock [26]. This region belongs to the temperate climate zone, which experiences four distinct seasons and is characterized by strong monsoon winds in spring, a warm and humid summer, a mild and cool autumn, and a dry and cold winter. The mean annual temperature is 4.9 °C and mean minimum and maximum air temperature are −21.5 and 32 °C, respectively. The total annual precipitation ranges from 600 to 800 mm, about 80% of which results from the rain during the summer months and the snow during the winter months, and the other 20% comes from hail and rime [27].

A typical land-use sequence in this region was selected, including over-mature mixed broadleaved-Korean pine forest, five secondary forests, and Korean pine plantation (KPP). See Figure 1 for seven forest types distribution. The over-mature forest (OMF) is dominated by Korean pine forest mixed with such deciduous species as *Betula* spp., *Populus* spp., *Quercus* spp., etc. The OMF, located at the mountain top, has not been disturbed by human activities. The secondary forests in the study area were classified into five types by dominant vegetation: Mongolian oak forest (MOF), mixed deciduous forest (MDF), *Betula platyphylla* forest (BPF), *Populus davidiana* forest (PDF), and hardwood forests (HWF) ranging in age from 60 to 66 years. They were regenerated naturally following the harvest of over-mature mixed broadleaved-Korean pine forest in 1949, 1950, 1950, 1950, and 1955, respectively. The 60-year-old pure Korean pine plantation was also converted from OMF by reforestation in 1965. Forest clearcutting slash disposal was carefully conducted, and all the surface litter and tree roots were removed from the clear-cut site before planting pure KPP. The secondary forests and KPP grew in a natural environment, and there was no human interference after reforestation. The seven forest types used for this study shared a similar history of the homogeneous substrate, topography, regional climate, and original vegetation. The basic characteristics of these forest types are summarized in Table 1.

Table 1. Characteristics of stands from which sample trees were harvested ^a.

Forest Type	Age (Year)	Main Species Composition ^b (Dominant Species)	Land-Use History	Areal Extent (ha)	Density (Trees ha ⁻¹)	BA (m ² ha ⁻¹)	DBH (cm)	
							Mean	Range
OMF	>160	(8), 9, 2, 3, 10, 11, 12, 13, 14	Natural forest	58.87	789	54.6	25.3	4.0–69.1
KPP	51	(8), 6, 3, 9, 5, 7, 6	Reforestation in 1965	2.3	2111	42.1	15.0	3.9–34.4
HWF	60	(4), (3), 2, (7)	Natural regeneration after clearcutting in 1955	2083.41	1578	26.2	10.1	1.6–50.3
BPF	65	(6), 15, 12, 17, 18	Natural regeneration after clearcutting in 1950	80.7	3022	25.4	7.4	1.4–34.8
PDF	65	(6), (5), 7, 4, 3, 2	Natural regeneration after clearcutting in 1950	44.4	1833	34.1	12.1	1.6–49.4
MDF	65	2, 7, 4, 3, 5, 6	Natural regeneration after clearcutting in 1950	99.47	2022	34.8	11.3	1.9–49.6
MOF	66	(1), 2, 3, 4, 5, 6	Natural regeneration after clearcutting in 1949	101.06	1511	36.6	13.7	2.0–55.4

^a Note: BA stands for the basal area; DBH for diameter at breast height; OMF for over-mature forest; KPP for Korean pine plantation; HWF for hardwood forest; BPF for *Betula platyphylla* forest; PDF for *Populus davidiana* forest; MDF for mixed deciduous forest; MOF for Mongolian oak forest. HWF, BPF, PDF, MDF, and MOF were five major secondary forests. ^b 1, *Quercus mongolica* Fisch.; 2, *Tilia amurensis* Rupr.; 3, *Fraxinus mandshurica* Rupr.; 4, *Phellodendron amurense* Rupr.; 5, *Populus davidiana* Dode.; 6, *Betula platyphylla* Suk.; 7, *Juglans mandshurica* Maxim.; 8, *Pinus koraiensis* Sieb. et Zucc.; 9, *Betula costata* Trautv. 10, *Acer ukurunduense* Trautv. et Mey; 11, *Abies nephrolepis* (Trautv.) Maxim; 12, *Ulmus laciniata* (Trautv.) Mayr; 13, *Acer tegmentosum* Maxim; 14, *Acer mono* Maxim; 15, *Larix gmelinii* Rupr.; 16, *Picea koraiensis* Nakai; 17, *Ulmus japonica* (Rehd.) Sarg; 18, *Alnus sibirica* Fisch. ex Turcz.

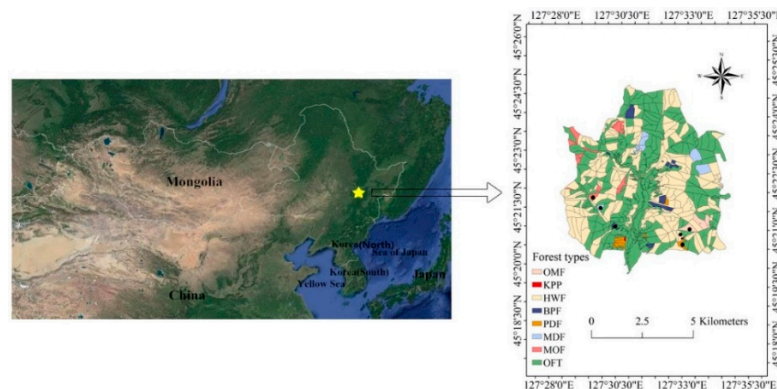


Figure 1. Map of the study site at the Maoershan Ecosystem Research Station of Northeast Forestry University in Northeast China (right map). The study site is located at the yellow pentacle of the left map. Seven black dots in the right map represent sampling sites of seven forest types. Abbreviation: OFT: other forest types (outside the seven forest types in present paper).

2.2. Soil Gas Flux Measurements

Fluxes of CH_4 , CO_2 , and N_2O were measured three times per month between 09:00 a.m. and 11:00 a.m. local time throughout the observation year using the static chamber-gas chromatography method. Stainless steel chambers of $50 \times 50 \times 50$ cm (length \times width \times height) were fabricated and equipped with two battery-operated fans of 10 cm in diameter for the mixing of air during the measurements. Two holes (2 cm in diameter) were drilled on the top of each chamber and fitted with rubber stoppers for headspace sampling [18]. One hole held a digital thermometer probe to measure the temperature in the chamber, and the other hole was used to collect the gas in the chamber. The experimental design was a randomized complete block design, and three replicated chambers were placed randomly at each site [16]. Each site was approximately 0.06 ha (20×30 m).

During the gas collection process, the chambers were inserted into permanently-installed stainless-steel lidless understructure ($0.5 \times 0.5 \times 0.2$ m), which had been fixed into the soil at a depth of 10 cm (we conducted field investigation and removed any shrubs or herbs within the chambers of 13 days before the first gas collection). Newly grown herbs were removed one day before collecting GHGs. The channel on top of the stainless-steel understructure was filled with water to make the system air-tight before the measurements [18].

Gas samples were collected at time intervals of 0, 10, 20, and 30 min after the chamber was placed in the plot using 50-mL hypodermic needles with three-way stopcocks. After being drawn, the gas samples were injected into pre-evacuated packs and brought to the laboratory for analysis to be conducted within one week using a gas chromatograph (GC, Agilent 7890A, Agilent Co., Santa Clara, CA, USA). To improve data quality, three measurements were selected for linear regression [18]. Sample sets were accepted when the linear regression was $r^2 > 0.90$ for all gases CH_4 , CO_2 , and N_2O [28].

2.3. Determination of Environmental Variables

When gas samples were collected, the interior air temperatures of the chamber, atmospheric environment temperatures and soil temperatures at 5 cm were recorded with digital thermometers (JM624, Jinming instrument CO. LTD, Tianjin, China). Soil volumetric water content ($\text{cm}^3 \text{H}_2\text{O cm}^{-3}$ soil) was also measured at 5 cm by a portable soil moisture tester (HS2, Campbell Scientific Inc, Logan, Utah, USA), which included a soil water sensor (MP-406B), a matched sampling connective rod, and a datalogger (MPM160 m, Campbell Scientific Inc, Logan, Utah, USA) [28].

A soil core, approximately 5 cm in diameter and 10 cm in length, was collected from each chamber location once per month during the monitoring year. Soil samples were transported on ice in an insulated cooler to the laboratory and stored in a refrigerator at $+4$ °C until analysis [13]. Soil

samples were analyzed within 48 h. All the soil samples had three replicates. The soil core was sieved to 2 mm. Soil pH was determined by a PHS-3S pH meter in suspensions composed of a 1:5 ratio of soil to water. Soil N content (NO_3^- and NH_4^+) were extracted with a 2 M KCl solution (soil:solution, 1:5) and then filtered through a 0.45 μm filter [29]. The extracted solutions were measured by AA3 Continuous Flow Analytical System. Soil organic carbon was analyzed using a multi-N/C 2100 analyzer (Analytic Jena AG, Jena, Germany).

2.4. Global Warming Potential

The global warming potential of soils under seven different vegetation types in present study were calculated as follows [30].

$$\text{GWP} = \text{CO}_2 + \text{N}_2\text{O} \times 298 + \text{CH}_4 \times 25. \quad (1)$$

The cumulative GHG fluxes (GWP) = GHG fluxes (GWP) per unit area \times areal extent.

2.5. GHG Flux Directions

It should be noted that throughout the paper, the movement of GHGs from soil to atmosphere is giving a positive sign, and from atmosphere to soil, it is giving a negative sign.

2.6. Data Analysis

The relationship between R_S and T was examined by using an exponential model

$$R_S = \alpha \times \exp^{\beta \times T}, \quad (2)$$

where R_S is the soil respiration ($\mu\text{mol CO}_2 \text{ m}^{-2} \text{ s}^{-1}$), T is the soil temperature at a depth of 5 cm, α and β are regression coefficients. Q_{10} is a quotient of change in R_S caused by change in temperature by 10 $^\circ\text{C}$, and can be indicative of the sensitivity of R_S to temperature. It is calculated as follows [31]:

$$Q_{10} = \exp^{10\beta}. \quad (3)$$

All the experimental data were calculated by averaging the measurements of the three replicates for each sampling. One-way ANOVA (Duncan comparison) was conducted to examine the difference in CH_4 , CO_2 , and N_2O fluxes among the seven forest types. Stepwise multiple linear regression was developed to quantify the response of the environmental variables to CH_4 , CO_2 , and N_2O fluxes in the seven forest types. We used a Bonferroni correction of $\alpha = 0.05/7 = 0.0071$ to adjust for multiple regression analysis, which is considered as “significant correlation” when it ranges from 0.0071 to 0.05. All the statistical analyses were carried out using SPSS version 17.0 software (SPSS, Inc. Chicago, IL, USA).

3. Results

3.1. Soil Properties

OMF and KPP had higher annual average air temperatures than those of the five secondary forests except for MOF, and OMF had a higher annual average soil temperature than that of the secondary forests by 0.30–3.03 $^\circ\text{C}$ and of KPP by 2.78 $^\circ\text{C}$ ($p < 0.05$, Table 2). The annual average soil moisture decreased in the following order: OMF > HWF > PDF > KPP > MDF > BPF > MOF ($p < 0.05$, Table 2). The soil pH of KPP was significantly higher than that of both OMF and the secondary forests ($p < 0.05$, Table 2). The concentrations of NO_3^- -N and NH_4^+ -N in KPP were significantly higher than those of OMF by 80.1% and 273.4%, and of secondary forests by 280.6%–795.4% and 385.3%–458.3%, respectively ($p < 0.05$, Table 2). The SOC in HWF soils was the highest among all the forest stands, and the SOC in OMF was significantly higher than that of KPP, PBF, and MOF by 30.3%, 38.6%, and 48.7%, respectively ($p < 0.05$, Table 2).

Table 2. Physico-chemical properties of experimental sites. Data are expressed as mean \pm SE, $n = 12$.

Properties	OMF	KPP	HWF	BPF	PDF	MDF	MOF
Air T ($^{\circ}$ C)	5.92 \pm 0.01B	5.63 \pm 0.01B	3.44 \pm 0.16E	4.79 \pm 0.02C	4.05 \pm 0.21D	4.93 \pm 0.05C	6.93 \pm 0.05A
Soil T ($^{\circ}$ C)	7.20 \pm 0.01A	4.42 \pm 0.01E	4.17 \pm 0.06F	5.24 \pm 0.07D	5.63 \pm 0.04C	5.17 \pm 0.15D	6.90 \pm 0.11B
Soil moisture (%)	35.45 \pm 0.49A	27.90 \pm 0.12C	34.42 \pm 0.33A	26.58 \pm 0.32D	30.84 \pm 0.41B	27.35 \pm 0.56D	23.96 \pm 0.47E
Soil pH	5.51 \pm 0.04C	6.02 \pm 0.03A	5.66 \pm 0.16B	5.43 \pm 0.05BC	5.47 \pm 0.24BC	5.53 \pm 0.06B	5.72 \pm 0.05B
NO ₃ ⁻ -N (mg kg ⁻¹)	5.42 \pm 0.35B	9.76 \pm 0.19A	2.58 \pm 0.26C	1.09 \pm 0.13D	2.22 \pm 0.42C	2.18 \pm 0.35C	1.98 \pm 0.20C
NH ₄ ⁺ -N (mg kg ⁻¹)	6.46 \pm 0.48B	24.12 \pm 2.32A	4.97 \pm 0.07B	4.95 \pm 0.66B	4.60 \pm 1.69B	4.38 \pm 0.75B	4.32 \pm 0.19B
Soil organic C (g kg ⁻¹)	72.02 \pm 7.25B	55.26 \pm 1.08CD	96.37 \pm 8.15A	51.96 \pm 3.32D	61.77 \pm 2.07BCD	69.92 \pm 4.52BC	48.42 \pm 2.37D

Note: The capital letters after numerical values indicate statistically significant differences within physico-chemical properties under different vegetation types ($p < 0.05$).

3.2. Seasonal Variation of GHG Fluxes

3.2.1. CH₄ Fluxes

It was observed that the CH₄ fluxes were negative with clear seasonal variations among the seven forest types. The experiment found that the highest CH₄ absorption peak occurred in summer while the lowest absorption peak occurred in winter (Figure 2). The CH₄ absorption from secondary forests was significantly higher than that of KPP by 32.6%–67.0% ($p < 0.05$) except for BPF, and it was recorded from MDF and MOF to be significantly higher than that of OMF and the other secondary forests during the sampling period ($p < 0.05$, Figure 2). Secondary forests averaged a higher CH₄ absorption by 19.6%–51.0% compared with OMF except for BPF (Figure 2). There was a significant difference ($p < 0.05$) in CH₄ absorption among the seven forest types during the non-growing season, whereas no significant difference was observed during the growing season ($p > 0.05$, Figure 2). The CH₄ absorption from OMF, KPP, and the five secondary forests during the growing season were 2.5 times, 5.5 times, and 1.7–3.2 times higher than that of the non-growing season, respectively (Figure 2).

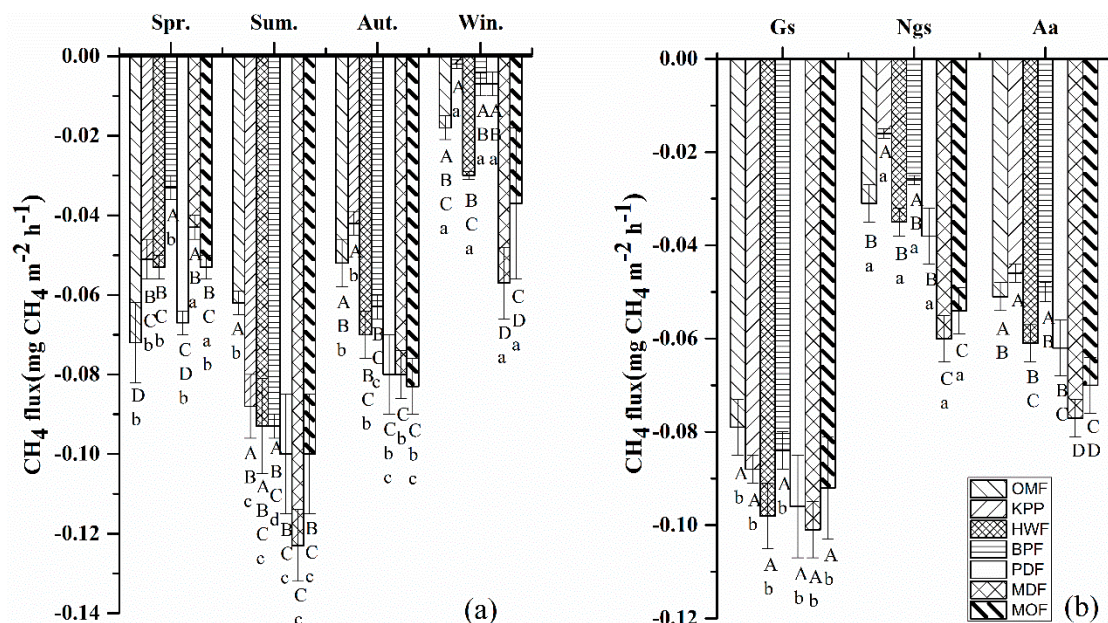


Figure 2. Seasonal variations (a), dynamics of Gs and Ngs (b), and the annual average (b) of methane fluxes from the over-mature forest, Korean pine plantation, and five secondary forests at the Maoershan Ecosystem Research Station in Northeast China. The lowercase letters indicate statistically significant differences within treatments among different seasons. The capital letters indicate statistically significant differences within seasons among different treatments. Abbreviations: Spr., Spring; Sum., Summer; Aut., Autumn; Win., Winter; Gs, Growing Season; Ngs, Non-growing Season; Aa, Annual Average.

Stepwise multiple regression analysis for CH₄ flux is as follows: in OMF, CH₄ fluxes had significant negative correlations with NH₄⁺-N ($p < 0.05$) and SOC ($p < 0.0071$). In KPP, CH₄ fluxes

had negative correlations with air temperature ($p < 0.0071$), and significant positive correlations with NO_3^- -N ($p < 0.05$). For the five secondary forests, CH_4 fluxes had significant positive correlations with air temperature, and negative correlations with soil temperature in HWF and MDF. In BPF, soil temperature, SVWC, and NO_3^- -N were the dominant factors controlling CH_4 fluxes ($p < 0.0071$). In PDF, CH_4 fluxes had significant negative correlations with air temperature ($p < 0.0071$), and in MOF, no significant relationships were observed between those environmental factors and CH_4 fluxes ($p < 0.1$) (Table 3).

Table 3. The driving factors of CH_4 , CO_2 , and N_2O fluxes in seven types of vegetation at the Maershan Ecosystem Research Station in Northeast China.

Plot	AT	ST	SVWC	pH	NO_3^- -N	NH_4^+ -N	SOC	Intercept	R^2	p
Models for soil CH_4										
OMF						−0.008 *	−0.005 **	0.587 *	0.663	<0.05
KPP	−0.002 **				0.004 *			−0.129 *	0.842	<0.0071
HWF	0.003 *	−0.007 **						−0.045 **	0.612	<0.05
BPF		−0.004 **	0.002 *		0.198 **			−0.117 *	0.927	<0.0071
PDF	−0.003 **							−0.047 **	0.626	<0.0071
MDF	0.004 *	−0.007 *						−0.057 **	0.441	<0.1
MOF								0.836	0.330	<0.1
Models for soil CO_2										
OMF		12.920 **	15.382 *					−512.687 *	0.891	<0.0071
KPP		21.477 **	−6.017 **					−476.729	0.973	<0.0071
HWF		16.692 **						114.102 **	0.833	<0.0071
BPF		23.067 **						57.177 *	0.895	<0.0071
PDF		25.094 **						2928.966 *	0.944	<0.0071
MDF		33.999 **					−10.888 *	454.856	0.936	<0.0071
MOF	−19.018 *	49.746 **			−112.542 *			388.194 **	0.943	<0.0071
Models for soil N_2O										
OMF					0.018 **			−0.068 *	0.851	<0.0071
KPP								0.016 *	0.018	nsc
HWF	0.01 *					0.009 *		−0.040	0.537	<0.05
BPF								0.005	0.284	<0.1
PDF				−0.121 *		−0.058 *		0.891 *	0.640	<0.05
MDF	0.001 **		−0.002 *	−0.155 **		−0.018 *		0.994 **	0.797	<0.05
MOF			0.001 *					−0.005	0.494	<0.05

Note: * indicates significant effects at $p < 0.05$; ** indicates significant effects at $p < 0.0071$; nsc indicates no significant correlation. AT, air temperature; ST, soil temperature.

3.2.2. CO_2 Fluxes

The CO_2 flux of each vegetation type was always positive with a clear seasonal variation. The highest emissions occurred in summer and the lowest emissions observed in winter for each site (Figure 3). The mean annual CO_2 fluxes from the five secondary forests throughout the sampling period were significantly higher than that from OMF by 32.9%–78.6% ($p < 0.05$). Secondary forests averaged a higher CO_2 flux by 14.1%–53.4% compared with KPP (Figure 3). For CO_2 fluxes, there were significant differences ($p < 0.05$) among OMF, KPP, and secondary forests in different seasons (Figure 3). The CO_2 emissions from OMF, KPP, and five secondary forests during the growing season were significantly higher than during the non-growing season by 1020.2%, 597.7%, and 382.6%–539.5%, respectively.

Stepwise multiple regression analysis showed that CO_2 fluxes, as measured from KPP, OMF, and secondary forests, were significantly positively correlated with soil temperature ($p < 0.0071$) (Table 3). The exponential models of R_5 against T explained 70%, 92%, and 39%–82% of the seasonal variability in R_5 in OMF, KPP, and five secondary forests (Figure 4). The Q_{10} values (the sensitivity of R_5 to temperature) for R_5 were 2.20, 3.16, 2.59, 2.92, 2.75, 2.32, and 1.93 in OMF, KPP, HWF, BPF, PDF, MDF, and MOF, respectively (Figure 4). In addition, Table 3 shows that CO_2 fluxes from OMF also had significant positive correlations with SVWC ($p < 0.05$). CO_2 fluxes from KPP also had significant negative correlations with SVWC ($p < 0.0071$). CO_2 fluxes from MDF also had significant negative correlations with SOC ($p < 0.05$). CO_2 fluxes from MOF also had significant negative correlations with air temperature and NO_3^- -N ($p < 0.05$) (Table 3).

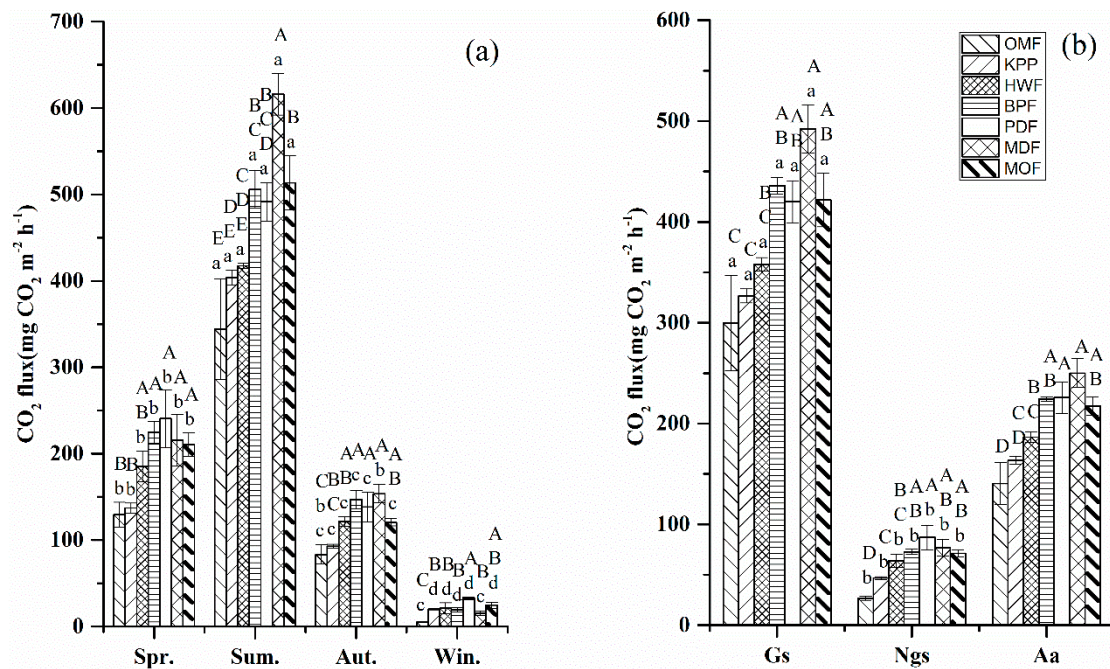


Figure 3. Seasonal variations (a), dynamics of Gs and Ngs (b), and the annual average (b) of carbon dioxide emissions from the over-mature forest, Korean pine plantation, and five secondary forests at the Maoershan Ecosystem Research Station in Northeast China. See Figure 2 for the explanation of the different lowercase letters and capital letters and the different abbreviations.

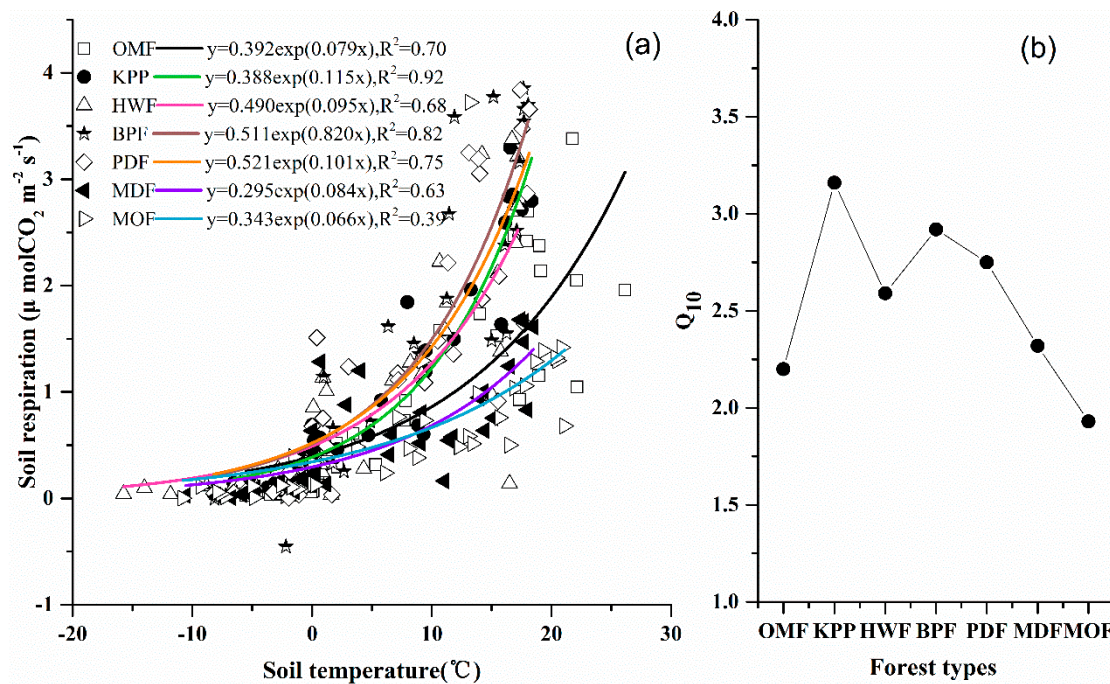


Figure 4. Relationships between soil respiration and soil temperature at a depth of 5 cm (a) and Q_{10} (b) for the seven forest stands.

3.2.3. N₂O Fluxes

The N₂O fluxes were always positive throughout the sampling period from OMF, KPP, and the five secondary forests. There were significant differences in N₂O fluxes in each observation season among the experimental forest types ($p < 0.05$). The N₂O fluxes in spring were significantly higher than

those in the other seasons except OMF ($p < 0.05$, Figure 5). According to the annual statistics, the N_2O fluxes decreased in the following order: MDF > OMF > KPP > PDF > HWF > MOF > BPF ($p < 0.05$). The N_2O fluxes from PDF and MOF were significantly lower than that of OMF by 59.9% and 35.9%, and of KPP by 59.0% and 34.4%, respectively ($p < 0.05$, Figure 5). However, for N_2O fluxes, there was no significant difference ($p > 0.05$) between OMF and KPP. The N_2O emissions from KPP, PDF, and MOF during the non-growing season were significantly higher than those during the growing season ($p < 0.05$, Figure 5).

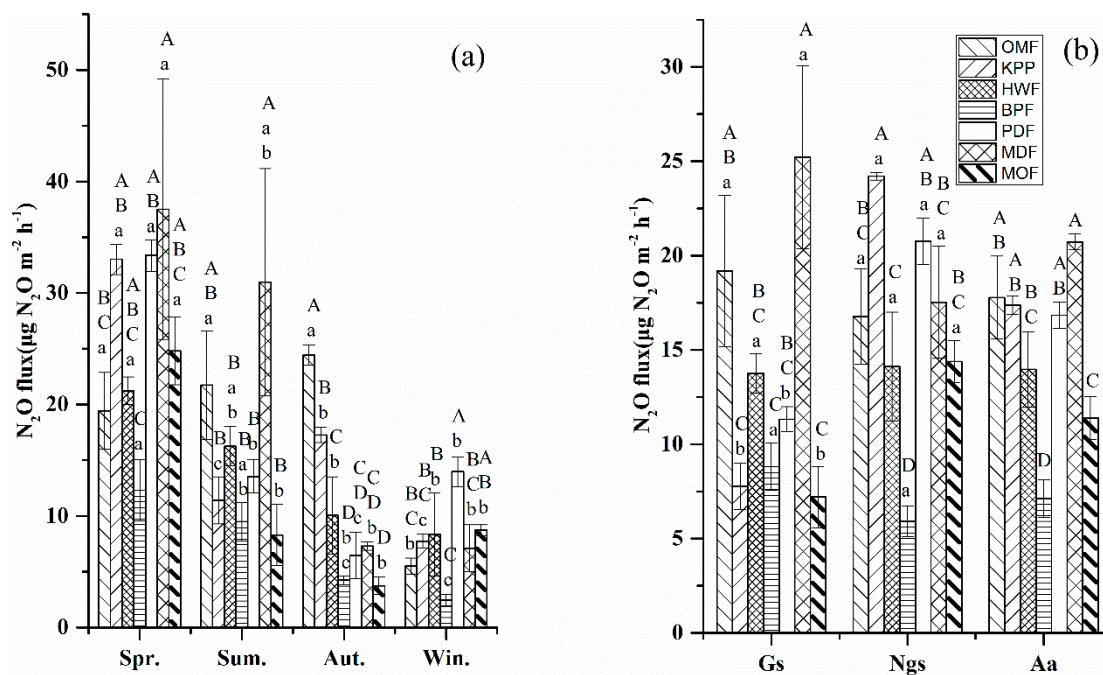


Figure 5. Seasonal variations (a), dynamics of Gs and Ngs (b), and the annual average (b) of nitrous oxide emissions from the over-mature forest, Korean pine plantation, and five secondary forests at the Maershan Ecosystem Research Station in Northeast China. See Figure 2 for the explanation of the different lowercase letters and capital letters and the different abbreviations.

From the stepwise multiple regression analysis for N_2O fluxes, in OMF, N_2O fluxes had positive correlations with $NO_3^- - N$ ($p < 0.0071$). However, no significant relationships were observed between those environmental factors and N_2O fluxes from KPP and BPF. N_2O fluxes from HWF had significant positive correlations with air temperature and $NH_4^+ - N$ ($p < 0.05$). The soil pH and $NH_4^+ - N$ were the dominant factors controlling N_2O fluxes from PDF ($p < 0.05$). In MDF, N_2O fluxes had significant negative correlations with SVWC, pH, and $NH_4^+ - N$, and a significant positive correlation with air temperature. A significant positive correlation was only observed between SVWC and N_2O fluxes from MOF (Table 3).

3.3. Estimation of GHG Emissions and GWPs

CH_4 fluxes varied from -4.12 (KPP) to -6.74 (MDF) $kg CH_4 ha^{-1} year^{-1}$ in different forest types (Figure 6). The cumulative CH_4 fluxes varied from -9.48 (KPP) to $-11,201.80$ (HWF) $kg CH_4 y^{-1}$. CO_2 fluxes varied from 12.46 (OMF) to 22.07 (MDF) $t CO_2 ha^{-1} year^{-1}$ in all the plots, and four secondary forest types (except for HWF) were significantly higher than that of KPP by 30.5%–50.1%, and five secondary forest types were 31.9%–77.1% greater than that of OMF ($p < 0.05$, Figure 6). The cumulative CO_2 fluxes increased in the order of Korean pine plantation ($33.80 t CO_2 year^{-1}$) < over-mature forest ($733.22 t CO_2 year^{-1}$) < secondary forest (885.19 – $34,230.43 t CO_2 year^{-1}$) (Table 4). They in the secondary forest were 55.7 and 1208.3 times higher than those in OMF and KPP, respectively. N_2O

fluxes varied from 0.62 (BPF) to 5.45 (OMF) kg N₂O ha⁻¹ y⁻¹ in all the plots, and they in OMF were significantly higher than those in OMF and secondary forests by 228.3% and 201.1%–779.0% ($p < 0.05$, Figure 6). The cumulative N₂O fluxes varied from 3.82 (KPP) to 2520.93 (HWF) kg N₂O year⁻¹. The total cumulative CH₄, CO₂, and N₂O fluxes were −13.37 t CH₄ year⁻¹, 41,608.96 t CO₂ year⁻¹, and 3.24 t N₂O year⁻¹ through the whole year in seven forest types at the Maoershan Ecosystem Research Station in Northeast China (Table 4).

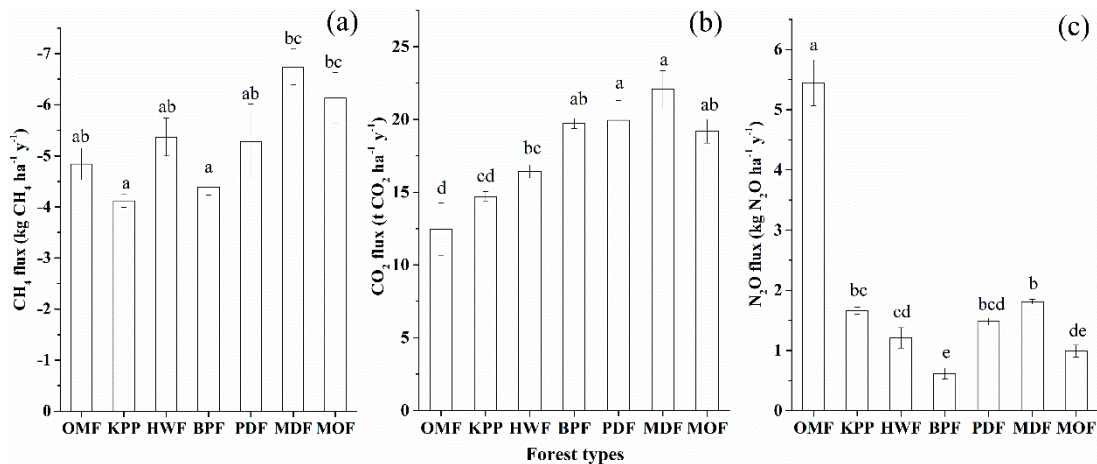


Figure 6. CH₄ fluxes (a), CO₂ fluxes (b), and N₂O fluxes (c) from the over-mature forest, Korean pine plantation and five secondary forests at the Maoershan Ecosystem Research Station in Northeast China. The lowercase letters indicate statistically significant differences among different treatments.

Table 4. Estimation of the cumulative GHG fluxes for each forest type at the Maoershan Ecosystem Research Station in Northeast China. Data are expressed as mean ± SE, $n = 3$.

Sites	Total CH ₄ Flux (kg CH ₄ year ⁻¹)	Total CO ₂ Flux (t CO ₂ year ⁻¹)	Total N ₂ O Flux (kg N ₂ O year ⁻¹)
OMF	−284.84 ± 18.32a (2.13%)	733.22 ± 105.79de (1.76%)	321.01 ± 22.60b (9.90%)
KPP	−9.48 ± 0.30a (0.07%)	33.80 ± 0.76e (0.08%)	3.82 ± 0.13b (0.12%)
HWF	−11,201.8 ± 774.17b (83.76%)	34,230.43 ± 915.36a (82.27%)	2520.93 ± 358.65a (77.75%)
BPF	−354.00 ± 13.36a (2.65%)	1591.67 ± 15.97bcd (3.83%)	50.57 ± 7.13b (1.56%)
PDF	−234.28 ± 32.66a (1.75%)	885.19 ± 60.78cde (2.13%)	65.86 ± 2.63b (2.03%)
MDF	−670.43 ± 34.61a (5.01%)	2194.97 ± 126.88b (5.28%)	180.37 ± 3.27b (5.56%)
MOF	−619.50 ± 50.34a (4.63%)	1939.68 ± 83.08bc (4.66%)	99.71 ± 10.04b (3.08%)
Total flux	−13,374.33 ± 841.90	41,608.96 ± 814.40	3242.27 ± 336.40

Note: The different lowercase letters after numerical values indicate statistically significant differences within GHG fluxes (CH₄, CO₂, and N₂O) under different forest types.

In the research presented in this paper, the GWP was computed based on the fluxes of CH₄, CO₂, and N₂O measured from soils. The GWP of different secondary forests varied from 16.66 t CO₂ eq. ha⁻¹ (HWF) to 22.44 t CO₂ eq. ha⁻¹ (MDF) (Table 5). However, five secondary forests averaged higher GWP by 33.7%–80.1% compared with OMF. Secondary forests, except for HWF, averaged a higher GWP by 31.6%–52.8% compared with KPP. Additionally, no significant differences were observed between OMF and KPP (Table 5). One-way ANOVA analyses revealed that there was a remarkable difference among seven forest types ($p < 0.05$, Table 5). The cumulative GWP increased in the order of Korean pine plantation (33.79 t CO₂ eq year⁻¹) < over-mature forest (733.26 t CO₂ eq year⁻¹) < secondary forest (898.95–34,702.67 t CO₂ eq year⁻¹) (Table 5). They in the secondary forest were 56.4 and 1224.8 times higher than those in OMF and KPP, respectively. CO₂ fluxes were the largest contributor for GWP in all land uses, while CH₄ and N₂O fluxes showed a minor contribution to GWP (Table 5). The total cumulative GWP was 42,151.87 t CO₂ eq year⁻¹ through the whole year in seven forest types at the Maoershan Ecosystem Research Station in Northeast China (Table 5).

Table 5. Estimation of Global Warming Potential (GWP) for each forest type at the Maoershan Ecosystem Research Station in Northeast China. Data are expressed as mean \pm SE, $n = 3$.

Sites	GWPCH ₄ (t CO ₂ eq. ha ⁻¹ year ⁻¹)	GWPCO ₂ (t CO ₂ eq. ha ⁻¹ year ⁻¹)	GWPN ₂ O (t CO ₂ eq. ha ⁻¹ year ⁻¹)	Total GWP (t CO ₂ eq. ha ⁻¹ year ⁻¹)	Cumulative GWP (t CO ₂ eq year ⁻¹)
OMF	-0.12 \pm 0.01ab	12.46 \pm 1.80d	1.63 \pm 0.11a	12.46 \pm 1.80d	733.26 \pm 105.80cd (1.74%)
KPP	-0.10 \pm 0.01a	14.70 \pm 0.33cd	0.49 \pm 0.02bc	14.69 \pm 0.33cd	33.79 \pm 0.76d (0.08%)
HWF	-0.14 \pm 0.01abc	16.43 \pm 0.44bc	0.36 \pm 0.05cd	16.66 \pm 0.38bc	34,702.67 \pm 794.28a (82.33%)
BPF	-0.11 \pm 0.01a	19.72 \pm 0.35ab	0.19 \pm 0.03e	19.80 \pm 0.22ab	1597.59 \pm 17.90bc (3.79%)
PDF	-0.13 \pm 0.02abc	19.94 \pm 1.37a	0.44 \pm 0.02bcd	20.25 \pm 1.40a	898.95 \pm 61.95cd (2.13%)
MDF	-0.17 \pm 0.01c	22.07 \pm 1.28a	0.54 \pm 0.01b	22.44 \pm 1.28a	2231.78 \pm 127.62b (5.29%)
MOF	-0.15 \pm 0.01bc	19.19 \pm 0.82ab	0.29 \pm 0.03de	19.33 \pm 0.80ab	1953.83 \pm 79.86b (4.64%)
Total					42,151.87 \pm 698.53

Note: The different lowercase letters after numerical values indicate statistically significant differences within GWP under different forest types.

4. Discussion

4.1. Factors Controlling GHG Fluxes

4.1.1. Methane

CH₄ fluxes showed similar seasonal patterns in seven forest types (CH₄ sink sites). This finding is in accordance with previous studies that the maximum CH₄ absorption value primarily occurred in summer and little emission value was found in the early spring at the same location [32], because the greater soil water environment due to the thawing of frozen soil in spring favors the production of an anaerobic environment. The anaerobic environment is beneficial to the methanogens' metabolic activities and leads to an increase in the production of CH₄ in spring [33]. Since the soil temperature increased gradually and reached the highest point in summer, some studies suggested that rising soil temperatures facilitated the consumption of CH₄ [16,34,35]. The CH₄ absorption value decreased with the decreasing soil temperature in winter. Soil temperature is an important controller of CH₄ consumption at temperatures between -5 and 10 °C [35]; 20 and 30 °C [36]; and between 20 and 30 °C [34], CH₄ consumption was greatly reduced below -5 °C as the low temperature significantly reduced microbial activities. However, it had a minimum soil temperature of about -16.4 °C below the 5 cm depth in winter in the present study, and thus the low temperature in winter is considered one of the factors for inducing low CH₄ absorption in forest soils. Furthermore, the snow cover and frozen soil in winter could indicate a decrease in the soil pore connectivity, which hinders the diffusion of CH₄ into the soil and leads to a lower uptake rate [13].

In this study, The CH₄ fluxes showed significant negative correlations with the air temperature ($p < 0.05$), the soil temperature ($p < 0.05$), and SVWC ($p < 0.05$) (Table 3). The results suggested that adequate soil moisture and high soil temperature are necessary to support the aerobic CH₄ consumption through the activity of methanotrophs in the soil [37]. In general, soil temperature and SVWC were the key factors that affected the activities of methanogens and methanotrophs as well as the permeability of atmospheric O₂ into the soils, which was closely related to the interplay between CH₄ production and consumption by oxidizing microorganisms [5,19]. The soil NO₃⁻-N and NH₄⁺-N content presented a primary effect on CH₄ fluxes in OMF, KPP, and BPF plots (Table 3). However, some studies found that the concentrations of NO₃⁻-N and NH₄⁺-N could reduce CH₄ fluxes while others reported opposite results [38,39]. This is because the interactions between the N and CH₄ cycle are complex and therefore involve various uncertainties [40]. In the present study, CH₄ from OMF exhibited a distinct negative correlation with SOC (Table 3). This is consistent with the previous conclusion that increased SOC continuously promotes CH₄ oxidation [19]. In addition, soil physico-chemical properties indicated significant differences due to different forest types (Table 2),

and stepwise multiple linear regression showed differences in CH₄ fluxes among different forest types depending on the comprehensive influence of the above factors.

4.1.2. Carbon Dioxide

It was observed that the CO₂ emissions were higher in summer as compared to winter during the monitoring of the seven vegetation types at the Maershan Ecosystem Research Station in Northeast China (Figure 3). Similar results were found by Dou et al. [16]. The Q₁₀ values for Soil respiration ranged from 1.93 to 3.16 across the seven forest ecosystems (Figure 4) and were consistent with the values previously reported for temperate forests (1.8–4.1) [41]. The Q₁₀ values showed the varied response of soil respiration to temperature among the seven forest stands. Additionally, soil respiration was controlled by soil temperature, and there was a positive correlation between them (Table 3). These results suggest that the proper soil temperature could promote the increase of microbial activities and then easily enhance mineralization of unavailable decomposable organic substrates [5], and there is a high rate of decomposition of soil organic C at high temperatures [42,43]. A significant negative correlation was discovered between CO₂ fluxes and the soil NO₃⁻-N in MOF (Table 3). The soil NO₃⁻-N can lead to carbon limitation, which has adverse effects on the nutrient supply of microorganisms. Moreover, soil nitrogen can reduce heterotrophic respiration by inhibiting decomposition of organic matter [44,45]. Additionally, there was a negative correlation between soil respiration rate and SOC in MDF. This is contrary to the finding that there was a significant positive correlation between soil respiration rate and soil organic C content in the forest system [46], which is because the soil organic C in the present study region was unable to provide adequate nutrition for soil organisms, leading to reduced biological activities and a slower respiration rate.

4.1.3. Nitrous Oxide

The N₂O fluxes were negligible in the seven forest soils, and the highest fluxes occurred in the spring; some peaks of N₂O emissions were observed in forest soils in the summer after rainfall (Figure 5). These results are aligned with other studies that showed low N₂O emission in the forest soils and an increase in N₂O emission rates after heavy rainfall [13,43]. This is also inconsistent with another study that showed the lowest N₂O flux appeared in the hot season while the peak N₂O flux appeared in the cold season in the afforested soils [16].

The thawing of the soil in the spring and heavy rainfall in the summer create slightly anaerobic conditions that lead to the emission of short-lived and intense N₂O fluxes due to the denitrification process in some anaerobic microsites in the soil [47]. The increasing soil temperatures could increase both nitrification [48,49] and denitrification [49]. In drier areas where moisture is limited, soil mineralization and nitrification could be stimulated by increased moisture contents [50]. However, in wetter areas, increased moisture contents may induce anaerobiosis, allowing N₂O production via denitrification [51]. Additionally, autotrophic nitrification could be inhibited by low soil pH [52], and denitrification rates are also generally decreased by acidity [52]. In OMF, abundant NO₃⁻-N provided sufficient substrates for denitrification. The increased concentrations of NH₄⁺ following harvest can stimulate nitrification and NO₃⁻ production [53]. The N₂O emissions were negatively correlated with NH₄⁺-N ($p < 0.05$) in PDF. The NH₄⁺ requirement of nitrifying microorganisms varies with the change of NH₄⁺ concentration. Therefore, the response of nitrification process is different at the concentration change of NH₄⁺ [54], which implies that NH₄⁺-N inhibits microbes via nitrification and N₂O emissions.

4.2. Effects of Different Forest Types on GHG Fluxes

Land use change is one of the most important factors that affect global warming. It affects the structure and function of ecosystem, changes the basic characteristic parameters of the soil surface, and influences the change of chemical composition in the atmosphere through the biogeochemical cycle, leading to the climate change [11,16,23]. In the present study, GHG fluxes varied considerably

among the seven forest types, suggesting the influence of the forest conversion on the rate of transport and emission of GHGs.

It was found that forest conversion significantly affects CH₄ absorption capacity in the present study (Figure 2). This finding is consistent with the previous conclusion that deforestation increased soil CH₄ absorption in various soils [1,55]. Deforestation is usually accompanied by considerable changes in soil properties (e.g., soil texture, soil C and N substrate availability), which consequently control soil CH₄ production and oxidation [56]. The shift in methanotrophic type is one of the factors that lead to a change in soil CH₄ oxidation [55], because the land use change greatly influences the methanotrophic community structure and activity [57]. In addition, it is also related to the plant allelopathy; there is a large group of monoterpene species in Pinaceae plants, which decompose into the soil through the roots and litter and have an inhibitory effect on CH₄ oxidation [36]. Maurer et al. [58] also found that the toxic compounds produced by conifer species could impede soil CH₄ oxidation. Thus, in the present research, it is inferred that KPP (conifer species) in the Maoershan region may limit soil CH₄ oxidation in the methanotroph community structure and accelerate CH₄ micro-emission.

In this study, different environmental factors, dependent on the forest stands, influenced the soil respiration in different ways. By the harvesting in the early growth stages of secondary forests and KPP, forest lost the canopy cover; water and heat balance changed fundamentally due to the sudden disappearance of the canopy. The intensifying sunlight would lead to the increase of soil surface evaporation and the acceleration of litter decomposition. The disturbance (movement, scratch, and compaction, etc.) of topsoil caused by logging leads to certain changes in soil microenvironment, microbial population structure, soil physical and chemical properties, such as soil porosity, soil aggregate structure, and soil water-stable aggregate structure [11]. Therefore, the soil under different trees possesses diverse soil C stability and hydrological conditions and hence has different degrees of influences on soil respiration [59,60]. SVWC in HWF was relatively higher than that in other secondary forest soils, and the CO₂ fluxes were lower than those from other secondary forests and KPP (Table 2 and Figure 2). This is caused by the soil water status, such as the soil with high water content in HWF, the poor soil permeability hindered the diffusive exchange of CO₂ between the soil and the atmosphere [37]. Consequently, differences in CO₂ fluxes among forests in our study suggest different environmental conditions among the seven forest types.

N₂O fluxes from forest soils are a complex process, which is not only controlled by environmental factors such as soil temperature and moisture [28], but also affected by factors such as N and C availability in soil, vegetation biomass [61], and microbial community dynamics. Furthermore, vegetation types can contribute differently to these factors [62]. Plant species differ in their ability to influence nitrification and denitrification processes. Plants can also affect the N₂O emission by modifying NH₄⁺, NO₃⁻, and C contents and by changing the partial O₂ pressure in the soil [63].

The total GWP was significantly higher in the secondary forest than that in OMF and KPP (Table 5). The GWP mainly consisted of more than 90% CO₂ flux, and the CO₂ flux was significantly higher in the secondary forest than that in OMF and KPP (Figure 6). This is within the range of 84%–99% contribution from CO₂ emission by Mu et al. [64]. Therefore, higher total GWP resulted from higher CO₂ flux in the secondary forest than that in OMF and KPP. Although N₂O flux was significantly higher in OMF than that in secondary forest and KPP (Figure 6), the N₂O flux accounted for 13.1% of GWP. This is within the range of 4% (agriculture) to 16% (undisturbed forest) from N₂O on GWP observed by Shrestha et al. [65]. Thus, the influence of N₂O flux was minor for GWP. Similar results were reported in other studies that CO₂ was the major contributor for GWP [66–68]. The GWP comparison of the seven forest types indicates that the effects of the early human activities have not been completely eliminated in the middle stage of KPP and secondary forests.

5. Conclusions

Greenhouse gas fluxes evaluated for forest conversion (the over-mature forests, Korean pine plantation, and five secondary forests) indicated that CH₄ uptake in MDF and MOF was significantly

higher than that in OMF. Secondary forests averaged a higher CO₂ flux by 32.9%–78.6% compared with OMF. The N₂O flux in BPF and MOF was lower than that in OMF. There was no significant difference in GHG fluxes between KPP and OMF. The above conclusions show that GHG fluxes in several 60-year-old secondary forest types after clearcutting have not recovered to the level of OMF, which requires continuous monitoring for a long time. The GWP in KPP is significantly less than the paddy field, orchard, and upland GWP, and it in the secondary forest it is less than the paddy field, orchard GWP [69], suggesting that forest is a more desirable land use in reducing global warming.

However, based on the GWP comparison of seven forest types, GHG fluxes from the soil, without taking into account the GHG absorption by plants, has led to the increase of GWP in the study area due to the forest conversion, which has caused the regional climate warming. Air and soil temperature, SVWC, pH, NO₃⁻-N, NH₄⁺-N, and SOC are the most influential variables affecting GHG fluxes among soil properties studied, which, if manipulated, can help in mitigating GHG emissions and GWP. These findings suggest that forest conversion has important effects on GHG emissions and GWP.

Further studies are required for the comparison of the GHG fluxes and GWP between over-mature forest, secondary forests, plantations (Mongolian pine plantation, Larch plantation, and so forth), and croplands to forecast which vegetation type is most similar to the over-mature forest in GHG emissions, and to estimate the GHG emissions and GWP of the whole study area.

Author Contributions: C.M. and B.W. conceived the general idea of the paper, supervised and conducted the laboratory and/or field observations and measurements. All authors analyzed and discussed the results; B.W. and C.M. wrote and revised the paper; C.M. reviewed the edited manuscript.

Funding: The authors wish to acknowledge financial assistance supported by the National Natural Science Foundation of China (41430639), and the National Key Research and Development Program of China (2017YFC0504102).

Acknowledgments: We would like to thank the Maoershan Ecosystem Research Station for the field experiment. We also would like to thank the reviewers and editors for their time and effort.

Conflicts of Interest: The authors declare no conflict of interest.

References

1. Lavoie, M.; Kellman, L.; Risk, D. The effects of clear-cutting on soil CO₂, CH₄, and N₂O flux, storage and concentration in two Atlantic temperate forests in Nova Scotia, Canada. *For. Ecol. Manag.* **2013**, *304*, 355–369. [[CrossRef](#)]
2. IPCC. *Climate Change 2013: The Physical Science Basis. Contribution of Working Group I to the Fifth Assessment Report of the Intergovernmental Panel on Climate Change*; Cambridge University Press: Cambridge, UK; New York, NY, USA, 2013.
3. Fariás, L.; Florez-Leiva, L.; Besoain, V.; Sarthou, G.; Fernández, C. Dissolved greenhouse gases (nitrous oxide and methane) associated with the naturally iron-fertilized Kerguelen region (KEOPS 2 cruise) in the Southern Ocean. *Biogeosci. Discuss.* **2015**, *11*, 12531–12569. [[CrossRef](#)]
4. Rowlings, D.W.; Grace, P.R.; Kiese, R.; Weier, K.L. Environmental factors controlling temporal and spatial variability in the soil-atmosphere exchange of CO₂, CH₄ and N₂O from an Australian subtropical rainforest. *Glob. Chang. Biol.* **2012**, *18*, 726–738. [[CrossRef](#)]
5. Li, Y.; Dong, S.; Liu, S.; Zhou, H.; Gao, Q.; Cao, G.; Wang, X.; Su, X.; Zhang, Y.; Tang, L.; et al. Seasonal changes of CO₂, CH₄ and N₂O fluxes in different types of alpine grassland in the Qinghai-Tibetan Plateau of China. *Soil Biol. Biochem.* **2015**, *80*, 306–314. [[CrossRef](#)]
6. IPCC. *Climate Change 1994: Radiative Forcing of Climate Change and an Evaluation of the IPCC IS92 Emissions Scenarios*; Cambridge University Press: Cambridge, UK; New York, NY, USA, 1995.
7. Ehhalt, D.; Prather, M. Atmospheric chemistry and greenhouse gases. In *Climate Change 2001: The Scientific Basis*; Cambridge University Press: London, UK, 2001; pp. 228–248.
8. Maljanen, M.; Hytönen, J.; Martikainen, P.J. Fluxes of N₂O, CH₄ and CO₂ on afforested boreal agricultural soils. *Plant Soil* **2001**, *231*, 113–121. [[CrossRef](#)]
9. IPCC. *Climate Change 2014: Impacts, Adaptation, and Vulnerability Working Group II Contribution to the Fifth Assessment Report*; Cambridge University Press: Cambridge, UK; New York, NY, USA, 2014.

10. Mills, R.T.E.; Dewhurst, N.; Sowerby, A.; Emmett, B.A.; Jones, D.L. Interactive effects of depth and temperature on CH₄ and N₂O flux in a shallow podzol. *Soil Biol. Biochem.* **2013**, *62*, 1–4. [[CrossRef](#)]
11. Benanti, G.; Saunders, M.; Tobin, B.; Osborne, B. Contrasting impacts of afforestation on nitrous oxide and methane emissions. *Agric. For. Meteorol.* **2014**, *198–199*, 82–93. [[CrossRef](#)]
12. Mishurov, M.; Kiely, G. Nitrous oxide flux dynamics of grassland undergoing afforestation. *Agric. Ecosyst. Environ.* **2010**, *139*, 59–65. [[CrossRef](#)]
13. Carmo, J.B.D.; Neto, E.R.D.S.; Duarte-Neto, P.J.; Ometto, J.P.H.B.; Martinelli, L.A. Conversion of the coastal Atlantic forest to pasture: Consequences for the nitrogen cycle and soil greenhouse gas emissions. *Agric. Ecosyst. Environ.* **2012**, *148*, 37–43. [[CrossRef](#)]
14. Maljanen, M.; Shurpali, N.; Hytönen, J.; Mäkiranta, P.; Aro, L.; Potila, H.; Laine, J.; Li, C.; Martikainen, P.J. Afforestation does not necessarily reduce nitrous oxide emissions from managed boreal peat soils. *Biogeochemistry* **2012**, *108*, 199–218. [[CrossRef](#)]
15. Lagomarsino, A.; Agnelli, A.E.; Pastorelli, R.; Pallara, G.; Rasse, D.P.; Silvennoinen, H. Past water management affected GHG production and microbial community pattern in Italian rice paddy soils. *Soil Biol. Biochem.* **2015**. [[CrossRef](#)]
16. Dou, X.; Zhou, W.; Zhang, Q.; Cheng, X. Greenhouse gas (CO₂, CH₄, N₂O) emissions from soils following afforestation in central China. *Atmos. Environ.* **2015**, *126*, 98–106. [[CrossRef](#)]
17. Ding, W.; Cai, Z.; Tsuruta, H. Methane concentration and emission as affected by methane transport capacity of plants in freshwater marsh. *Water Air Soil Pollut.* **2004**, *158*, 99–111. [[CrossRef](#)]
18. Sun, X.; Mu, C.; Song, C. Seasonal and spatial variations of methane emissions from montane wetlands in Northeast China. *Atmos. Environ.* **2011**, *45*, 1809–1816. [[CrossRef](#)]
19. Tate, K.R. Soil methane oxidation and land-use change—from process to mitigation. *Soil Biol. Biochem.* **2015**, *80*, 260–272. [[CrossRef](#)]
20. Konda, R.; Ohta, S.; Ishizuka, S.; Heriyanto, J.; Wicaksono, A. Seasonal changes in the spatial structures of N₂O, CO₂, and CH₄ fluxes from Acacia mangium plantation soils in Indonesia. *Soil Biol. Biochem.* **2010**, *42*, 1512–1522. [[CrossRef](#)]
21. Priemé, A.; Christensen, S. Natural perturbations, drying–wetting and freezing–thawing cycles, and the emission of nitrous oxide, carbon dioxide and methane from farmed organic soils. *Soil Biol. Biochem.* **2001**, *33*, 2083–2091. [[CrossRef](#)]
22. Wang, C.K.; Yang, J.Y.; Zhang, Q.Z. Soil respiration in six temperate forests in China. *Glob. Chang. Biol.* **2006**, *12*, 2103–2114. [[CrossRef](#)]
23. Shi, B.; Gao, W.; Jin, G. Effects on rhizospheric and heterotrophic respiration of conversion from primary forest to secondary forest and plantations in northeast China. *Eur. J. Soil Biol.* **2015**, *66*, 11–18. [[CrossRef](#)]
24. Chen, D.K.; Zhou, X.F.; Zhao, H.X.; Wang, Y.H.; Jing, Y.Y. *Study on the Structure, Function and Succession of the Four Types in Natural Secondary Forest*; Northeast Forestry University Press: Harbin, China, 1982.
25. Smith, K.A.; Dobbie, K.E.; Ball, B.C.; Bakken, L.R.; Sitaula, B.K.; Hansen, S.; Brumme, R.; Borken, W.; Christensen, S.; Priemé, A.; et al. Oxidation of atmospheric methane in Northern European soils, comparison with other ecosystems, and uncertainties in the global terrestrial sink. *Glob. Chang. Biol.* **2010**, *6*, 791–803. [[CrossRef](#)]
26. Wang, C.K. Biomass allometric equations for 10 co-occurring tree species in Chinese temperate forests. *For. Ecol. Manag.* **2006**, *222*, 9–16. [[CrossRef](#)]
27. Wang, X.; Wang, C.; Guo, Q.; Wang, J. Improving the CO₂ storage measurements with a single profile system in a tall-dense-canopy temperate forest. *Agric. For. Meteorol.* **2016**, *228–229*, 327–338. [[CrossRef](#)]
28. Tang, X.; Liu, S.; Zhou, G.; Zhang, D.; Zhou, C. Soil-atmospheric exchange of CO₂, CH₄, and N₂O in three subtropical forest ecosystems in southern China. *Glob. Chang. Biol.* **2006**, *12*, 546–560. [[CrossRef](#)]
29. Li, M.; Zhou, X.; Zhang, Q.; Cheng, X. Consequences of afforestation for soil nitrogen dynamics in central China. *Agric. Ecosyst. Environ.* **2014**, *183*, 40–46. [[CrossRef](#)]
30. IPCC. *Climate Change 2007: Synthesis Report*; Cambridge University Press: Cambridge, UK; New York, NY, USA, 2007.
31. Shi, B.; Jin, G. Variability of soil respiration at different spatial scales in temperate forests. *Biol. Fertil. Soils* **2016**, *52*, 561–571. [[CrossRef](#)]
32. Liu, S. Effluxes of Soil Carbon Dioxide, Methane and Nitrous Oxide in Four Chinese Temperate Forests. Master's Thesis, Northeast Forestry University, Harbin, China, 2010. (In Chinese).

33. Yang, G.; Chen, H.; Wu, N.; Tian, J.; Peng, C.; Zhu, Q.; Zhu, D.; He, Y.; Zheng, Q.; Zhang, C. Effects of soil warming, rainfall reduction and water table level on CH₄ emissions from the Zoige peatland in China. *Soil Biol. Biochem.* **2014**, *78*, 83–89. [[CrossRef](#)]
34. Nesbit, S.P.; Breitenbeck, G.A. A laboratory study of factors influencing methane uptake by soils. *Agric. Ecosyst. Environ.* **1992**, *41*, 39–54. [[CrossRef](#)]
35. Castro, M.S.; Steudler, P.A.; Melillo, J.M.; Aber, J.D.; Bowden, R.D. Factors controlling atmospheric methane consumption by temperate forest soils. *Glob. Biogeochem. Cycles* **1995**, *9*, 1–10. [[CrossRef](#)]
36. Geng, S.C.; Chen, Z.J.; Zhang, J.H.; Lou, X.; Wang, X.X.; Dai, G.H.; Han, S.J.; Yu, D.D. Soil methane fluxes of three forest types in Changbai Mountain of Northeast China. *Chin. J. Ecol.* **2013**, *32*, 1091–1096.
37. Wu, X.; Yao, Z.; Brüggemann, N.; Shen, Z.Y.; Wolf, B.; Dannenmann, M.; Zheng, X.; Butterbach-Bahl, K. Effects of soil moisture and temperature on CO₂ and CH₄ soil–atmosphere exchange of various land use/cover types in a semi-arid grassland in Inner Mongolia, China. *Soil Biol. Biochem.* **2010**, *42*, 773–787. [[CrossRef](#)]
38. Aronson, E.L.; Helliiker, B.R. Methane flux in non-wetland soils in response to nitrogen addition: A meta-analysis. *Ecology* **2010**, *91*, 3242–3251. [[CrossRef](#)] [[PubMed](#)]
39. Yonemura, S.; Nouchi, I.; Nishimura, S.; Sakurai, G.; Togami, K.; Yagi, K. Soil respiration, N₂O, and CH₄ emissions from an Andisol under conventional-tillage and no-tillage cultivation for 4 years. *Biol. Fertil. Soils* **2014**, *50*, 63–74. [[CrossRef](#)]
40. Bodelier, P.L. Interactions between nitrogenous fertilizers and methane cycling in wetland and upland soils. *Curr. Opin. Environ. Sustain.* **2011**, *3*, 379–388. [[CrossRef](#)]
41. Xu, M.; Qi, Y. Spatial and Seasonal Variations of Q₁₀ Determined by Soil Respiration Measurements at a Sierra Nevada Forest. *Glob. Biogeochem. Cycles* **2001**, *15*, 687–696. [[CrossRef](#)]
42. Almaraz, J.J.; Zhou, X.; Mabood, F.; Madramootoo, C.; Rochette, P.; Ma, B.L.; Smith, D.L. Greenhouse gas fluxes associated with soybean production under two tillage systems in southwestern Quebec. *Soil Tillage Res.* **2009**, *104*, 134–139. [[CrossRef](#)]
43. Jain, N.; Arora, P.; Tomer, R.; Mishra, S.V.; Bhatia, A.; Pathak, H.; Chakraborty, D.; Kumar, V.; Dubey, D.S.; Harit, R.C.; et al. Greenhouse gases emission from soils under major crops in Northwest India. *Sci. Total Environ.* **2016**, *542 Pt A*, 551. [[CrossRef](#)]
44. Weintraub, M.N.; Schimel, J.P. Interactions between carbon and nitrogen mineralization and soil organic matter chemistry in Arctic tundra soils. *Ecosystems* **2003**, *6*, 129–143. [[CrossRef](#)]
45. Wang, Q.K.; Wang, S.L.; He, T.X.; Liu, L.; Wu, J.B. Response of organic carbon mineralization and microbial community to leaf litter and nutrient additions in subtropical forest soils. *Soil Biol. Biochem.* **2014**, *71*, 13–20. [[CrossRef](#)]
46. Bae, K.; Lee, D.K.; Fahey, T.J.; Woo, S.Y.; Quaye, A.K.; Lee, Y.K. Seasonal variation of soil respiration rates in a secondary forest and agroforestry systems. *Agrofor. Syst.* **2013**, *87*, 131–139. [[CrossRef](#)]
47. Gomes, J.; Bayer, C.; Costa, F.D.S.; Piccolo, M.D.C.; Zanatta, J.A.; Vieira, F.C.B.; Six, J. Soil nitrous oxide emissions in long-term cover crops-based rotations under subtropical climate. *Soil Tillage Res.* **2009**, *106*, 36–44. [[CrossRef](#)]
48. Goodroad, L.L.; Keeney, D.R. Nitrous oxide production in aerobic soils under varying pH, temperature and water content. *Soil Biol. Biochem.* **1984**, *16*, 39–43. [[CrossRef](#)]
49. Castaldi, S. Responses of nitrous oxide, dinitrogen and carbon dioxide production and oxygen consumption to temperature in forest and agricultural light-textured soils determined by model experiment. *Biol. Fertil. Soils* **2000**, *32*, 67–72. [[CrossRef](#)]
50. Levine, J.S.; Cofer, W.R.; Sebach, D.I.; Winstead, E.L.; Sebach, S.; Boston, P.J. The effects of fire on biogenic soil emissions of nitric oxide and nitrous oxide. *Glob. Biogeochem. Cycles* **1988**, *2*, 445–449. [[CrossRef](#)]
51. Teepe, R.; Brumme, R.; Beese, F.; Ludwig, B. Nitrous oxide emission and methane consumption following compaction of forest soils. *Soil Sci. Soc. Am. J.* **2004**, *68*, 605–611. [[CrossRef](#)]
52. Dalal, R.C.; Wang, W.; Robertson, G.P.; Parton, W.J. Nitrous oxide emission from Australian agricultural lands and mitigation options: A review. *Aust. J. Soil Res.* **2003**, *41*, 165–195. [[CrossRef](#)]
53. Vitousek, P.M.; Matson, P.A.; Cleve, K.V. Nitrogen availability and nitrification during succession: Primary, secondary and old-field seres. *Plant Soil* **1989**, *115*, 229–239. [[CrossRef](#)]
54. Gao, W.; Kou, L.; Zhang, J.; Müller, C.; Yang, H.; Li, S. Ammonium fertilization causes a decoupling of ammonium cycling in a boreal forest. *Soil Biol. Biochem.* **2016**, *101*, 114–123. [[CrossRef](#)]

55. Tate, K.R.; Ross, D.J.; Saggar, S.; Hedley, C.B.; Dando, J.; Singh, B.K.; Lambie, S.M. Methane uptake in soils from *Pinus radiata* plantations, a reverting shrubland and adjacent pastures: Effects of land-use change, and soil texture, water and mineral nitrogen. *Soil Biol. Biochem.* **2007**, *39*, 1437–1449. [[CrossRef](#)]
56. Zhou, M.; Wang, X.; Ren, X.; Zhu, B. Afforestation and deforestation enhanced soil CH₄ uptake in a subtropical agricultural landscape: Evidence from multi-year and multi-site field experiments. *Sci. Total Environ.* **2019**, *662*, 313–323. [[CrossRef](#)]
57. Kolb, S. The quest for atmospheric methane oxidizers in forest soils. *Environ. Microbiol. Rep.* **2009**, *1*, 336–346. [[CrossRef](#)]
58. Maurer, D.; Kolb, S.; Haumaier, L.; Borken, W. Inhibition of atmospheric methane oxidation by monoterpenes in Norway spruce and European beech soils. *Soil Biol. Biochem.* **2008**, *40*, 3014–3020. [[CrossRef](#)]
59. Sheng, H.; Yang, Y.; Yang, Z.; Chen, G.; Xie, J.; Guo, J.; Zou, S. The dynamic response of soil respiration to land-use changes in subtropical China. *Glob. Chang. Biol.* **2010**, *16*, 1107–1121. [[CrossRef](#)]
60. Xu, X.; Zou, X.; Cao, L.; Zhamangulova, N.; Zhao, Y.; Tang, D.; Liu, D. Seasonal and spatial dynamics of greenhouse gas emissions under various vegetation covers in a coastal saline wetland in southeast China. *Ecol. Eng.* **2014**, *73*, 469–477. [[CrossRef](#)]
61. Yamulki, S.; Anderson, R.; Peace, A.; Morison, J.I.L. Soil CO₂ CH₄ and N₂O fluxes from an afforested lowland raised peatbog in Scotland: Implications for drainage and restoration. *Biogeosciences* **2013**, *10*, 7623–7630. [[CrossRef](#)]
62. Dusenbury, M.P.; Engel, R.E.; Miller, P.R.; Lemke, R.L.; Wallander, R. Nitrous oxide emissions from a Northern Great Plains soil as influenced by nitrogen management and cropping systems. *J. Environ. Qual.* **2008**, *37*, 542. [[CrossRef](#)] [[PubMed](#)]
63. Ghosh, S.; Majumdar, D.; Jain, M.C. Nitrous oxide emissions from kharif and rabi legumes grown on an alluvial soil. *Biol. Fertil. Soils* **2002**, *35*, 473–478. [[CrossRef](#)]
64. Mu, Z.; Kimura, S.D.; Hatano, R. Estimation of global warming potential from upland cropping systems in central Hokkaido, Japan. *Soil Sci. Plant Nutr.* **2010**, *52*, 371–377. [[CrossRef](#)]
65. Shrestha, R.K.; Lal, R.; Penrose, C. Greenhouse Gas Emissions and Global Warming Potential of Reclaimed Forest and Grassland Soils. *J. Environ. Qual.* **2009**, *38*, 426–436. [[CrossRef](#)]
66. Jauhainen, J.; Silvennoinen, H.; Hämäläinen, R.; Kusin, K.; Limin, S.; Raison, R.J.; Vasander, H. Nitrous oxide fluxes from tropical peat with different disturbance history and management. *Biogeosciences* **2012**, *9*, 1337–1350. [[CrossRef](#)]
67. Melling, L.; Hatano, R.; Goh, K. Global warming potential from soils in tropical peatland of Sarawak, Malaysia. *Phyton* **2005**, *45*, 275–284.
68. Ishikura, K.; Darung, U.; Inoue, T.; Hatano, R. Variation in Soil Properties Regulate Greenhouse Gas Fluxes and Global Warming Potential in Three Land Use Types on Tropical Peat. *Atmosphere* **2018**, *9*, 465. [[CrossRef](#)]
69. Ruan, L. Greenhouse Gases Emissions from Different Land Use Types and Their Global Warming Potential at Xianning, Hubei, China. Master's Thesis, Huazhong Agricultural University, Wuhan, China, 2007. (In Chinese).

